HHS Public Access

Author manuscript

Mol Cell Neurosci. Author manuscript; available in PMC 2016 September 01.

Published in final edited form as:

Mol Cell Neurosci. 2015 September ; 68: 36–45. doi:10.1016/j.mcn.2015.03.016.

Differential Targeting of Dynamin-1 and Dynamin-3 to Nerve Terminals During Chronic Suppression of Neuronal Activity

Barbara Calabrese[*] and **Shelley Halpain**[*]

Division of Biological Sciences, and Sanford Consortium for Regenerative Medicine, University of California San Diego, La Jolla, California, United States

Abstract

Neurons express three closely related dynamin genes. Dynamin 1 has long been implicated in the regulation of synaptic vesicle recycling in nerve terminals, and dynamins 2 and 3 were more recently shown also to contribute to synaptic vesicle recycling in specific and distinguishable ways. In cultured hippocampal neurons we found that chronic suppression of spontaneous network activity differentially regulated the targeting of endogenous dynamins 1 and 3 to nerve terminals, while dynamin 2 was unaffected. Specifically, when neural activity was chronically silenced for 1–2 weeks by tetrodotoxin (TTX), the clustering of dynamin 1 at nerve terminals was reduced, while the clustering of dynamin 3 significantly increased. Moreover, dynamin 3 clustering was induced within hours by the sustained blockade of AMPA receptors, suggesting that AMPA receptors may function to prevent Dyn3 accumulation within nerve terminals. Clustering of dynamin 3 was induced by an antagonist of the calcium-dependent protein phosphatase calcineurin, but was not dependent upon intact actin filaments. TTX-induced clustering of Dyn3 occurred with a markedly slower time-course than the previously described clustering of synapsin 1. Potassium-induced depolarization rapidly de-clustered dynamin 3 from nerve terminals within minutes. These results, which have implications for homeostatic synapse restructuring, indicate that the three dynamins have evolved different regulatory mechanisms for trafficking to and from nerve terminals in response to changes in neural activity.

Keywords

synaptic vesicle; membrane trafficking; endocytosis; homeostatic plasticity; tetrodotoxin; calcineurin

Introduction

The dynamins comprise a family of GTPases that are involved in membrane fission events (Ferguson and De Camilli, 2012; Mettlen et al., 2009). All three closely related dynamin

[*]**Authors for correspondence:** Division of Biological Sciences, University of California San Diego & Sanford Consortium for Regenerative Medicine, 2880 Torrey Pines Scenic Drive, La Jolla, CA 92037-0695, United States, bcalabrese@ucsd.edu (B. Calabrese), shalpain@ucsd.edu (S. Halpain).

genes are expressed in neurons (Cook et al., 1996), raising the possibility that they might participate in distinct cellular functions. At the synapse, the function of dynamin 1 (Dyn1) in presynaptic vesicle endocytosis has been well characterized. Dyn1 accumulates at clathrin coated endocytic pits, polymerizes into a collar-like structure at the neck of the endocytic bud, and mediates GTP hydrolysis dependent vesicle fission. This vesicle membrane retrieval, recycling of vesicle membrane, and subsequent re-loading of neurotransmitter, ensures the continuous supply of vesicles for sustained neurotransmission.

Dyn2 is ubiquitously expressed in tissue throughout the organism and is not up-regulated during synaptogenesis (Cook et al., 1996). Dyn2 is thought to support synaptic transmission in Dyn1 and Dyn3 double knock-out mice (Raimondi et al., 2011), and regulates the recycling of synaptic vesicles with kinetics and properties that distinguish it from Dyn1 and 3 (Tanifuji et al., 2013). Dyn2 is also implicated in additional functions, such as non-clathrin mediated endocytosis and microtubule related activities (Gonzalez-Jamett et al., 2013; Ishida et al., 2011).

Compared to dynamins 1 and 2, Dyn3 has been relatively less well characterized since its initial discovery in the brain (Cook et al., 1996). Dyn3 was proposed to be a component of the postsynaptic compartment of rat hippocampal neurons (Gray et al., 2003; Gray et al., 2005). However, studies using genetic knockdown and direct physiological measurements of neurotransmission support a presynaptic role for endogenous Dyn3 in synaptic vesicle recycling (Raimondi et al., 2011; Tanifuji et al., 2013). In Dyn1 knockout mice Dyn3 accumulates at nerve terminals, and defects in synaptic vesicle endocytosis are more severe in the Dyn1/Dyn3 double knockout mouse than in the Dyn1 single knockout mouse (Ferguson et al., 2007; Raimondi et al., 2011), suggesting that they have some redundant functions. Nevertheless, the degree to which Dyn3 functions overlap with those of Dyn1 remains unclear.

A recent study demonstrated that the three dynamin isoforms have distinguishable features at the synapse of rat superior cervical ganglion neurons (Tanifuji et al., 2013). Dyn1 regulated vesicle recycling to the readily releasable pool with fast kinetics and within in a relatively slow time window (>50 ms) in a manner dependent upon action potential frequency. By comparison Dyn3 resupplied the readily releasable pool of vesicles with slower kinetics but more rapidly, within 20 ms of the incoming action potential, and in a manner *in*dependent of firing frequency. Dyn2 displayed properties intermediate between the other two isoforms (Tanifuji et al., 2013).

In the present study we compared the endogenous subcellular distribution of the three dynamin isoforms in cultured rat hippocampal neurons following chronic suppression of network activity. We observed that silencing of synaptic activity resulted in opposite effects on the presynaptic accumulation of Dyn1 and Dyn3, while having no detectable effect on Dyn2. These results indicate that dynamic changes in action potential firing rate can alter the ratio of Dyn1 and Dyn3 in nerve terminals, a finding that may have implications for synaptic function and homeostatic mechanisms.

Results

Subcellular distribution of the three dynamin isoforms

Tissue-wide expression of all three dynamin isoforms in the brain was previously described using northern blot analysis (Cook et al., 1996) and immunodetection (Urrutia et al., 1997). We used dissociated cultures derived from embryonic rat hippocampus to examine the subcellular distribution of the three dynamins and their response to neural activity. All evaluations were performed on cultures fixed after 21 days in vitro, at which time cultures have established near maximal synapse density and their glutamatergic synapses are mainly present on dendritic spines. As described previously (Calabrese et al., 2006), presynaptic terminals appear as small varicosities distributed along the dendrites, and are frequently found in close apposition to dendritic spines. Other nerve terminals are present at GABAergic inhibitory synapses along the dendrite. Each of the antibodies used to specifically detect the three dynamin isoforms was previously reported to lack crossreactivity to the other two isoforms (Gray et al., 2003; Kurklinsky et al., 2011; Lu et al., 2007). We confirmed in hippocampal neurons the selectivity of the Dyn1 and Dyn3 antibodies (Supplemental Fig. S1). All neurons in culture displayed specific immunostaining with all three antibodies; astrocytes were variably labeled with the three antibodies and were not examined further in this study.

Under control conditions we detected endogenous Dyn1 immunoreactivity in axons and nerve terminals, but also to some extent in dendrites and cell bodies (Fig. 1A, *left*), in agreement with previous findings (Faire et al., 1992; Noda et al., 1993). Dyn1 was distributed in a punctate manner along the dendritic arbor. Dyn1 puncta were strongly colocalized with the synaptic vesicle marker synapsin 1 (Syn1) (Fig. 1B), consistent with the known enrichment of both proteins within nerve terminals (McPherson et al., 1994).

In comparison to Dyn1, Dyn2 immunoreactivity appeared more evenly and diffusely distributed along axons and dendrites, and, although detectable, it lacked strong enrichment at synapses (Fig. 1A, *control*). Consistent with this observation, Dyn2 immunoreactivity was only weakly colocalized with Syn1, (Fig. 1B, *control*).

Similar to Dyn1, Dyn3 immunoreactivity in control cultures was characterized by a punctate staining pattern; however, for Dyn3 the puncta size was highly variable (Fig. 1A, *control*). Although a few large puncta colocalized with Syn1 (Fig. 1B, *control*) most puncta appeared to be small in size, and mainly distributed along the axon shaft, rather than being concentrated in axonal varicosities.

Chronic silencing of action potentials by TTX differentially alters Dyn1 and Dyn3 distribution patterns

All three dynamin isoforms have a role in the recycling of neurotransmitter vesicles at synapses (Raimondi et al., 2011; Tanifuji et al., 2013). Changes in the levels of action potential firing can alter the concentrations of synaptic proteins, including those that regulate vesicle retrieval (Cremona and De Camilli, 1997; Gundelfinger et al., 2003). Here we asked whether suppression of spontaneous electrical activity for various times would regulate the distribution of Dyn1, Dyn2, and Dyn3 at synapses. We chronically silenced spontaneous

network activity by culturing the neurons for two weeks in the presence of tetrodotoxin (TTX, 1μM), during which time synapses are being established and stabilized. In agreement with previous reports (Robinson et al., 1994), Dyn1 immunoreactivity became less prominent at synapses (Fig. 1A, *bottom row*) and became more diffusely distributed along axons. In opposite fashion, chronic TTX caused Syn1 to accumulate at synapses, as reported previously (Chi et al., 2001). Therefore, chronic TTX induced a prominent decrease in the colocalization of Dyn1 and Syn1 at synapses. We detected no change in the distribution of Dyn2.

Interestingly, this same prolonged block of action potential firing that decreased clustering of Dyn1 instead increased the clustering of Dyn3. TTX induced a redistribution of Dyn3 from a more diffusely punctate pattern to one where Dyn3 became concentrated in larger clusters (Fig. 1A, *bottom row*). These larger Dyn3-positive clusters strongly colocalized with Syn1, indicating that Dyn3 accumulated within nerve terminals (Fig. 1B, *bottom row*). The increase in colocalization was further enhanced because Syn1 itself also accumulated within nerve terminals.

We took a closer look at these unanticipated results for Dyn3. Qualitatively it appeared that in control conditions the majority of Dyn3 puncta were very small and diffusely distributed throughout the region where axons come into close proximity to dendrites and form synaptic contacts. These small puncta mostly did not overlap with the MAP2 signal, which is confined to the dendrite shaft. Instead, the majority of puncta appeared to be present within the meshwork of fine-caliber axons that typically wrap around the dendritic arbor of cultured hippocampal neurons (Fig. 2A, B control). Upon incubation with TTX for 2 weeks, these small puncta were greatly diminished in number, while at the same time larger puncta became more prominent (Fig. 2A, B TTX).

These qualitative observations were corroborated by quantitative analyses. First, the average coefficient of variation in pixel intensity over the image field was significantly increased in the presence of TTX (Fig. 2C). This result is consistent with the observation that after TTX there is a greater variation in signal intensity across the image compared to the control condition, where signal intensity is more uniform throughout each field of view, due to the diffuse distribution of small Dyn3-positive puncta throughout the axonal meshwork. Second, the average area occupied by individual puncta (defined as being between 6 and 18 pixels in size) was dramatically increased following TTX (Fig. 2D). This is again consistent with the qualitative observation of a reduction in small puncta concomitant with an increase in large puncta. Indeed, examination of a frequency histogram plotting the number of puncta per field across a range of sizes revealed a clear rightward shift in the size distribution, with TTX favoring puncta greater than 10 pixels at the expense of those under 10 pixels (Fig. 2E).

Taken together, these observations suggest that TTX induces a relocalization of Dyn3 from clusters within the axonal shaft to larger clusters within nerve terminals. The aggregated Dyn3 clusters now colocalize strongly with Syn1, which also accumulates within terminals after chronic action potential silencing.

TTX-induced Dyn3 clusters are located presynaptically

The above observation that Dyn3 can become highly concentrated in nerve terminals in an activity-dependent manner was somewhat unexpected, firstly because Dyn3 behaved oppositely to its close homolog Dyn1, and secondly because an earlier paper had indicated that Dyn3 was specifically enriched in dendritic spines, the postsynaptic compartment of excitatory synapses, rather than in the presynaptic terminal (Gray et al., 2003). We therefore evaluated more precisely which compartment (presynaptic or postsynaptic) corresponded to the large Dyn3 puncta that become prominent following TTX-induced action potential silencing. We observed that the large Dyn3 clusters were often adjacent to the tip of dendritic spines, where their fluorescence distributions partially overlapped at some, but not all, spines (Supplemental Fig. S2). We interpret this distribution pattern as indicating a selective presynaptic enrichment. However, to confirm this we carried out a series of three-dimensional reconstructions of deconvolved digital images from cultures that were double-labeled for Dyn3 together with either the specific presynaptic marker Syn1, or the specific postsynaptic markers Homer1c and Homer 2a (Fig. 3). Deconvolution methods are well-suited to visualize the relative spatial overlap of pre- and post-synaptic markers in vitro. Neuronal axons and dendrites in dissociated culture lie nearly flat in two dimensions along the coverslip surface, and photons emanating from closely-spaced locations can accurately be ‘reassigned’ to their point of origin based on the point-spread-function of the optical system used. A 90° rotation of the deconvolved x-y image to view it in the x-z dimension readily confirmed that the spatial location of Dyn3 and Syn1 substantially overlapped, consistent with their co-existence within the same presynaptic compartment (Fig. 3A). Furthermore, colocalization between endogenous Dyn3 and Syn1 was significantly greater than was colocalization between Dyn3 and Homer2, a postsynaptic marker, which, as expected, did not show significant overlap with Syn1 (Fig. 3B). Spatial overlap between Syn1 and Homer 1c was likewise very low (Fig. 3), consistent with their known segregation into presynaptic versus postsynaptic compartments, respectively. These observations were confirmed quantitatively by measuring the “coefficient of colocalization” (see the Experimental Methods section for details) for each of the above antibody combinations (Fig. 3D).

AMPA receptor blockade rapidly induces clustering of Dyn3

Long term incubation with TTX can induce multiple changes in neuronal structure and function (Pozo and Goda, 2010). We therefore examined the time course of TTX-induced Dyn3 clustering, and also asked whether glutamate receptor blockers had similar effects. Although we could detect a significant increase in the Dyn3 cluster area with a 72 hour incubation in TTX, we detected no significant change at shorter times of either 4 h or 12 h (Fig. 4). Action potential silencing therefore appears to induce a relatively slow accumulation of Dyn3 clusters at nerve terminals.

Interestingly, however, incubation of neuronal cultures with the AMPA receptor antagonist DNQX for only 4 h was sufficient to induce a significant increase in Dyn3 cluster area (Fig. 4). This may indicate that whatever mechanisms contribute to driving Dyn3 out of nerve terminals may be more readily triggered by activity at AMPA receptors specifically than by generalized neuronal depolarization *per se*.

TTX-induced Dyn3 clustering is slower than Syn1 clustering

Previous studies have established that Syn 1 accumulates in nerve terminals during suppression of action potential firing. We therefore asked whether TTX-induced Dyn3 and Syn1 accumulation occurred with a similar time course, which might implicate similar molecular mechanisms for their trafficking. However, we observed that Syn1 reached maximal levels of synapse accumulation within 1 h in the presence of TTX, whereas Dyn3 took several days to reach maximal accumulation (Fig. 5).

Dyn3 clustering is reversible and independent of F-actin

To address whether Dyn3 clustering is reversible we first incubated the cells with TTX for 2 weeks to induce Dyn3 clusters, then applied 20 mM KCl for 5 min to depolarize the neurons. Depolarization induced rapid de-clustering of Syn1 (Fig. 6A and B), in agreement with previous studies (Chi et al., 2001). Depolarization similarly induced declustering of Dyn3 within 5 min, suggesting that action potential firing and/or AMPA receptor activation may actively prevent the accumulation of Dyn3 within nerve terminals.

Filamentous actin (F-actin) tethers and organizes many protein complexes within specific subcellular domains (Calabrese et al., 2006; Cingolani and Goda, 2008). Moreover, F-actin is involved in endocytic mechanisms in nerve terminals and also binds to Syn1 (Nelson et al., 2013). However, disruption of the F-actin network using the actin assembly inhibitor latrunculin-A (LatA), which sequesters actin monomers, fails to disrupt synaptic vesicle clustering or recycling (Bleckert et al., 2012; Cesca et al., 2010). We therefore asked whether the TTX-induced increase in clustering of Dyn3 might be dependent upon an intact actin cytoskeleton. We first confirmed that pre-incubation of cultures with LatA (50 μM, 20 min) effectively eliminated F-actin, as detected using phalloidin staining (Suppl Fig. S3). In agreement with previous studies, LatA did not induce declustering of Syn1 (Fig. 6A). Similarly, LatA did not detectably alter the TTX-induced Dyn3 clusters (Fig. 6A and B), suggesting that the Dyn3 accumulation induced by silencing does not rely on intact actin filaments.

Calcineurin mediates Dyn3 clustering

A plausible mechanism through which neural activity might affect Dyn3 redistribution is via an increase in intracellular calcium, which in turn alters cell signaling events such as phosphorylation and dephosphorylation. Calcineurin is a calcium-dependent phosphatase that is activated during action potential firing and that is known to dephosphorylate Dyn1 (Cousin and Robinson, 2001) and Dyn2 (Chircop et al 2011). To test whether calcineurin regulates the accumulation of Dyn3 in nerve terminals, we treated 21 DIV hippocampal neurons for 1 hour with 0.5 μM ascomycin, a calcineurin inhibitor. Under this condition, Dyn3 redistributed into larger clusters (Fig. 7), similar to what we observe during action potential silencing by TTX.

Discussion

Synaptic vesicle membranes undergo bidirectional trafficking to and from the active zone of the presynaptic terminals and boutons of neurons (Bonanomi et al., 2006; Dittman and

Ryan, 2009). The endocytic retrieval and recycling of synaptic vesicle membrane occur via three main stages: assembly of a clathrin coat, membrane invagination, and membrane fission. Dynamin is a GTPase-containing protein that mediates this final critical step.

Three dynamin isoforms are products of three distinct genes that encode proteins sharing ~80% sequence homology (Urrutia et al., 1997). They differ particularly within their C-terminal region, which contain a proline-rich domain that is proposed to mediate their differential targeting and function (Cao et al., 1998; van der Bliek, 1999). All three dynamins are present in the nervous system; Dyn2 is ubiquitously expressed across tissues, while Dyn1 and Dyn3 are selectively enriched in the brain, with Dyn3 present at lower concentrations than Dyn1 (Cao et al., 1998; Ferguson et al., 2007; Gray et al., 2003). In this study we focused our efforts on Dyn1 and Dyn3, since Dyn2 displayed a fairly diffuse distribution across all compartments of the neuron, and did not relocalize in response to TTX. The central finding from our study is that Dyn1 and Dyn3 are differentially regulated in their presynaptic targeting during prolonged silencing of neuronal excitation. Dyn1 became less concentrated within nerve terminals, but Dyn3 became strikingly enriched in nerve terminals during chronic action potential silencing by TTX or by briefer periods of AMPA receptor silencing using DNQX. We discuss the implications of these findings below.

Dyn3 enrichment in nerve terminals

Previous reports indicated that Dyn3 might play a role mainly within the postsynaptic dendritic spine compartment (Gray et al., 2003; Gray et al., 2005), and subsequent studies based on GFP-tagged versions of Dyn3 implicated it in glutamate receptor trafficking in spines (Lu et al., 2007). However, later studies clearly demonstrated that all three dynamins, including Dyn3, play roles in regulating synaptic vesicle endocytosis (Raimondi et al., 2011; Tanifuji et al., 2013). Therefore, given that the subcellular distribution of Dyn3 remained uncertain, we carefully determined whether the TTX-induced synaptic enrichment we observed for Dyn3 was due to its presence in nerve terminals, dendritic spines, or both. By using image deconvolution methods, we were able to make an unambiguous conclusion that in our dissociated hippocampal cultures, Dyn3 becomes enriched within the presynaptic compartment in response to TTX, not within the postsynaptic dendritic spine compartment. We therefore conclude that, although Dyn3 may play a role in postsynaptic functions, it is likely to play a significant role within nerve terminals, especially under conditions of reduced neural activity.

Mechanisms regulating the targeting of Dyn3 to nerve terminals

We propose that the TTX-induced clustering of Dyn3 in nerve terminals is due to its relocalization from a diffuse collection of small clusters present throughout the axon. This conclusion is based on our observations that a) the average cluster area increases, b) the coefficient of variation in image intensity decreases (consistent with smaller clusters converting to bigger clusters) and c) the frequency distribution of Dyn3 cluster sizes shifts such that smaller clusters decrease and larger clusters increase in frequency. Interestingly, TTX-induced clusters, which accumulate over many hours, were rapidly dispersed within minutes by potassium-induced depolarization. This suggests that ongoing excitatory

neurotransmission and/or action potentials may normally drive Dyn3 out of the nerve terminal, where it otherwise accumulates when neurons are quiescent.

The mechanism for the accumulation of Dyn3 within the nerve terminal does not appear to require intact actin filaments, since TTX-induced clusters were not disrupted by incubation with the actin assembly inhibitor latrunculin A. Dyn3 must, therefore, anchor to some other assembly, potentially synaptic vesicles or non-actin based scaffolds, in order to be retained at the synapse. Such actin-independence is also observed for synaptic vesicle clusters within nerve terminals, since actin depolymerization does not induce dispersal of synaptic vesicles (Zhang and Benson, 2002).

The mechanism that permits Dyn3 to accumulate within nerve terminals does appear, however, to require phosphorylation, since inhibition of the protein phosphatase calcineurin was observed to stimulate Dyn3 clustering. These observations suggest a model in which nerve terminal depolarization induces Dyn3 dephosphorylation perhaps by activation of calcineurin, which then disrupts the delivery or anchoring of Dyn3 within the presynaptic compartment. Further studies are clearly needed to probe the molecular mechanisms for Dyn3 trafficking at synapses.

It is curious that TTX has opposite effects on Dyn1 vs Dyn3, because both molecules are regulated by calcineurin-dependent dephosphorylation (Cousin and Robinson, 2001). Endogenous Dyn1 is phosphorylated in synaptosome fractions at multiple sites; however phosphorylation at Ser 774 and Ser 778 accounts for the majority of phosphorylation (Graham et al., 2007), and evidence suggests that Ser-774 may be the most critical site for regulation of synaptic vesicle endocytosis (Smillie and Cousin, 2005). Both these sites are conserved in Dyn3 (Graham et al., 2007) (but Ser 774 is absent in Dyn2), and phosphorylation was detected at both these sites on Dyn3 present in synaptosome preparations (Graham et al., 2007). Cyclin dependent kinase 5 (cdk5), which is constitutively active in nerve terminals, appears to be the main protein kinase that phosphorylates Dyn3 in vivo (Smillie and Cousin, 2005), and under control conditions Dyn1 (Tan et al., 2003). Upon membrane depolarization, Dyn1 is dephosphorylated by calcineurin, at sites Ser 774/778 (Xue et al., 2011). Since these residues are present in Dyn3, it seems likely that Dyn3 is also dephosphorylated upon neuronal depolarization, and that this drives Dyn3 away from the nerve terminal.

The mechanism by which dephosphorylation might prevent Dyn3 from accumulating in nerve terminals is unclear. Calcineurin-mediated dephosphorylation of Dyn1 at Ser 774/778 reportedly increases its association with other proteins within the nerve terminal, and reduces its concentration in cytosol (Liu et al., 1994; Marks and McMahon, 1998; Presek et al., 1992). Our observations indicate that this model might not apply to Dyn3, however, since instead we observe that Dyn3 accumulates when calcineurin activity is blocked. It would be highly informative to identify the protein kinase and protein phosphatase signaling pathways that regulate Dyn3 trafficking at synapses, to identify Dyn3 binding partners, and to conduct structure-function analyses to determine whether and how analogous dephosphorylation events might have differential effects on the synaptic targeting of Dyn1 versus Dyn3.

The trafficking of other synaptic vesicle-associated proteins, including synapsin 1, also is regulated by neural activity and phosphorylation state (Chi et al., 2001; Cijsouw et al., 2014; Fernandez-Alfonso et al., 2006; Fortin et al., 2005; Verstegen et al., 2014). Several proteins involved in synaptic vesicle endocytosis, including alpha-adaptin, clathrin, amphiphysin 1 and epsin 1, diffuse away from nerve terminals during incubation with TTX as observed for Dyn1 (Bauerfeind et al., 1997; Mueller et al., 2004; Raimondi et al., 2011). It was therefore surprising to observe that Dyn3 instead accumulated within nerve terminals. In contrast to endocytic machinery proteins, several non-endocytic synaptic vesicle-associated proteins, including Munc18-1 (Cijsouw et al., 2014), alpha-synuclein (Fortin et al., 2005), and Syn1 (Chi et al., 2001), increase within nerve terminals following TTX, in parallel with increased synaptic vesicle numbers. The fact that Dyn3 traffics into nerve terminals similar to these vesicle proteins raises the intriguing question of whether Dyn3 may have some non-endocytic role in synaptic vesicle regulation that remains to be identified.

It seems likely that the specific mechanisms that increase the clustering of Syn1 at nerve terminals during TTX-induced silencing differ from those for Dyn3 clustering, since their time-courses differed so radically. TTX-induced Syn1 clustering reached maximal levels within 1 hour, but Dyn3 clustering reaching maximum several days later. This suggests that Syn1 and Dyn3 are unlikely to be delivered to nerve terminals within the same molecular complex. Nevertheless, at this point we cannot rule out that Syn1 and Dyn3 share similar trafficking mechanisms but display different kinetics due, for example, to differences in their relative abundance and/or saturation of their docking sites within the nerve terminal.

Effect of TTX versus DNQX: a clue to the trigger for Dyn3 relocalization?

From our initial data we postulated that Dyn3 accumulation within the nerve terminal is prevented by depolarization of the nerve terminal, potentially mediated by the calcium-dependent protein phosphatase calcineurin. TTX thus permits Dyn3 accumulation (or stimulates its active delivery) by blocking nerve terminal depolarizations. Based on this model, we had predicted that other means of silencing network activity in the cultures would mimic the effect of TTX in inducing Dyn3 to move to the synapse. Indeed, incubation with the AMPA receptor antagonist DNQX also induced Dyn3 enrichment at nerve terminals. Interestingly, however, the effect of DNQX was much more rapid than TTX, inducing a significant increase in Dyn3 clustering within hours, compared to the three days or more required for TTX to induce a similar degree of clustering. The reason for this substantial difference in the time course of Dyn3 relocalization is not known; however, it may provide a clue to the nature of the signal that initiates Dyn3 clustering.

Although TTX and DNQX both suppress depolarizations and ‘silence’ neuronal networks, they do so via distinct mechanisms. TTX blocks voltage-dependent sodium channels, and thus prevents action potentials from reaching nerve terminals and directing neurotransmitter release. In contrast, DNQX suppresses action potential firing by preventing synaptic transmission at glutamate receptors, thereby reducing depolarization and thus shifting the balance of excitation/inhibition in a neuronal network to favor inhibition. In addition, unlike TTX, DNQX silences miniature excitatory postsynaptic potentials that stem from spontaneous vesicle fusion in the absence of membrane depolarization (Han and Stevens,

2009; O'Brien et al., 1998). Our observation that DNQX was more efficient than TTX in inducing Dyn3 clustering could suggest that AMPA receptor activation is somehow coupled to a mechanism that prevents Dyn3 accumulation in nerve terminals. This influence of AMPA receptor activity might be additive to depolarization-dependent mechanisms, or could possibly provide the sole critical signal to drive Dyn3 away from terminals. In any case, such an AMPA receptor-dependent signal might reflect either AMPA receptors residing on the nerve terminal membrane, or retrograde signaling initiated by AMPA receptors on the post-synaptic neuron. AMPA receptor-mediated retrograde signals are indeed known to occur in the context of various forms of synapse regulation, including homeostatic synaptic plasticity (Wondolowski and Dickman, 2013).

Functional impact of activity-dependent trafficking of Dyn3

The TTX-induced accumulation of Dyn3 in the presynaptic compartment is concomitant with a declustering of Dyn1, suggesting that inactivity induces a “switch” of dynamin isoform within the nerve terminal. Recent studies suggest that this may have specific consequences for synaptic function. It has been somewhat unclear whether Dyn1 and Dyn3 serve identical functions in any or all subcellular compartments. Studies in knockout mice clearly demonstrate that Dyn3 can substitute for at least some functions of Dyn1 in the context of synaptic vesicle endocytosis (Raimondi et al., 2011; Tanifuji et al., 2013). However, although all three dynamin isoforms may exhibit substantial functional redundancy (Raimondi et al., 2011), the details of their functionality may differ.

A recent study provided strong evidence that Dyn1, Dyn2, and Dyn3 differentially regulate the kinetics and firing rate dependence of synaptic vesicle recycling (Tanifuji et al., 2013). One clear prediction from our results, therefore, is that the properties of synaptic vesicle retrieval will differ in neurons that have undergone a period of quiescence compared to those that have been recently active. For example, the “inactivity-dependent” switch from Dyn1 to Dyn3 should, according to the results of Tanifuji et al., (2013), cause nerve terminals to resupply their readily releasable pool more quickly. This switch may prepare the synapse to respond efficiently to a burst of action potentials by ensuring that neurotransmitter release is well-primed, despite a period of recent inactivity.

Such homeostatic synaptic plasticity mechanisms, which maintain an overall balance of excitation and inhibition in neural circuits in the face of changing activity patterns, are critical for a functionally stable nervous system (Turrigiano et al., 1998). Disrupted homeostatic plasticity has been implicated in brain disorders ranging from epilepsy to autism (Wondolowski and Dickman, 2013). The differential regulation of Dyn1 and Dyn3 that we have described here may function to help maintain homeostasis in presynaptic function by altering the properties of synaptic vesicle dynamics during changes in synapse activity rates.

Experimental Methods

Hippocampal cultures

Hippocampi were removed from embryonic day 18 (E18) Wistar rat brains, then treated with 9U/ml papain (Worthington) for 20 min, followed by trituration with a pipette. Dissociated neurons were plated on poly- L-lysine-coated 12-mm cover glasses at a density of 100 cells/mm^2 and maintained in neurobasal medium (NB; 21103-049, GIBCO), supplemented with B27 (17504-044, Invitrogen) and 0.5 mM L-glutamine (G7513, Sigma). Neurons were transfected with GFP-tagged Dyn1 and Dyn3 at 20 days in vitro (DIV) using calcium phosphate precipitation.

Drug treatments

TTX (1 μM), DNQX (20 μM), and ascomycin (0.5 μM) were obtained from Sigma. During long term applications the drugs were replenished every 4 days. The different incubation times described in the paper refer to the time interval prior fixing the cells at 21 DIV.

Immunocytochemistry

Neurons were fixed with 3.7% formaldehyde in phosphate buffered saline (PBS) plus 120 mM sucrose for 20 min at 37 °C. After washing three times with PBS for 10 min, neurons were permeabilized with 0.2% Triton X-100 in a buffer solution containing 100 mM Pipes Na, 1mM EGTA, 1mM MgCl2, 1% BSA plus 100 mM NH4Cl, pH 6.8 for 2 min at room temperature. After rinsing they were blocked for 1h with 10% Normal Goat Serum (NGS) diluted in the same buffer solution without NH4Cl. Mouse monoclonal anti-synapsin antibody at 1:200 (Chemicon), anti-Homer 1:500 (gift of dr. K. Furuichi), and mouse monoclonal MAP2 antibody HM2 at 1:5000 (Sigma), were incubated for 1h at room temperature and, following rinsing, incubated with AlexaFluor-568-conjugated secondary antibody (Molecular Probes) for 45 min at 37 °C. To label F-actin, AlexaFluor-568-phalloidin at 1:1000 (Molecular Probes) was incubated for 2h at room temperature in the presence of 2% BSA. Endogenous Dynamins were detected incubating the cells for 1h at room temperature with rabbit polyclonal Dyn1 and 2 antibodies at 1:1000 (kind gift of Dr. S. Schmid), and rabbit polyclonal Dyn3 at 1:3000 (kind gift from Dr. M. McNiven). This anti-Dyn3 antibody is suitable for detecting Dyn3 in rat tissue (Gray et al; 2003; Lu et al., 2007; Kurlinsky et al., 2011), but not in mouse tissue (Raimondi et al., 2011), perhaps because the primary amino acid sequence for Dyn3 differs between mouse and rat in the region to which the anti-peptide antibody was reportedly raised (Cao et al., 1998). All dynamin antibodies used in this study were previously characterized to exclude any crossreactivity across the various isoforms (Cao et al., 1998; Gray et al., 2003; Kurklinsky et al., 2011; Liu et al., 2008; Lu et al., 2007).

Imaging acquisition and quantitative image analysis

Optical sections (11 sections at 0.1 μm each) were acquired with an Olympus Fluoview 500 confocal microscope by sequential illumination using the 488 line of an argon laser, the HeNe Green 543 laser, and the HeCd 442 laser using a 60 ×1.4 NA Plan APO oil immersion objective.

Image deconvolution & coefficient of colocalizaton—For experiments in Fig. 3 we used a Deltavision deconvolution imaging system (Applied Precision, Inc), with an Olympus IX70 microscope, 60× 1.4 NA oil immersion objective, and CH350 camera. A z-series of specimen images were acquired at 0.2μm intervals in widefield mode. Deltavision software running on a Silicon Graphics O2 workstation was used to deconvolve the sample images by comparison to a pointspread function (PSF) acquired under identical imaging conditions using a point source (50nm diameter microbeads labeled with fluorophores of appropriate wavelengths). An Imaris software package (Bitplane, Zurich, Switzerland) was used to display fluorescently labeled objects as isosurface renderings, generate and animate rotations for the regions of interest, and calculate colocalization coefficients for the 3D-deconvolved images.

Quantification of Dyn3 and Syn1 cluster area—Using MetaMorph imaging software (Universal Imaging Corporation, WestChester, PA), confocal images were thresholded to highlight clusters according to user-defined settings, using the same image display settings for all treatment groups within an experiment. Cluster area was calculated automatically by the MetaMorph software. Partial clusters at the margins of the image were excluded from analysis.

Coefficient of variation—The coefficient of variation was calculated as the ratio between the standard deviation over the mean of pixel intensity values within regions of fixed size selected randomly along both the distal and proximal region of the dendritic arbor. All measurements were expressed as mean ± SEM.

Statistics

Statistical significance was set at the 95% confidence level (two-tailed) and calculated using Prism (Graphpad Software, La Jolla, CA, USA). Values are presented as mean ± SEM and were derived from repetitions of at least three independent culture preparations. Statistical tests and numbers of neurons or synapses for each assay are defined in the corresponding figure legends. Pharmacological experiments were statistically compared with their corresponding vehicle control experiments.

Supplementary Material

Refer to Web version on PubMed Central for supplementary material.

Acknowledgments

We thank Dr. S. Schmid for the Dyn1 construct and Dyn1 and 2 antibodies, and Dr. M. McNiven for the Dyn3 construct and antibody. We thank Kathy Spencer and William B Kiosses for assistance with quantitative image analysis. This work was supported by NIH grants MH087823 and NS37311.

References

Bauerfeind R, Takei K, De Camilli P. Amphiphysin I is associated with coated endocytic intermediates and undergoes stimulation-dependent dephosphorylation in nerve terminals. Journal of biological chemistry. 1997; 272:30984–30992. [PubMed: 9388246]

Bleckert A, Photowala H, Alford S. Dual pools of actin at presynaptic terminals. Journal of neurophysiology. 2012; 107:3479–3492. [PubMed: 22457456]

Bonanomi D, Benfenati F, Valtorta F. Protein sorting in the synaptic vesicle life cycle. Progress in neurobiology. 2006; 80:177–217. [PubMed: 17074429]

Calabrese B, Wilson MS, Halpain S. Development and regulation of dendritic spine synapses. Physiology. 2006; 21:38–47. [PubMed: 16443821]

Cao H, Garcia F, McNiven MA. Differential distribution of dynamin isoforms in mammalian cells. Molecular biology of the cell. 1998; 9:2595–2609. [PubMed: 9725914]

Cesca F, Baldelli P, Valtorta F, Benfenati F. The synapsins: key actors of synapse function and plasticity. Progress in neurobiology. 2010; 91:313–348. [PubMed: 20438797]

Chi P, Greengard P, Ryan TA. Synapsin dispersion and reclustering during synaptic activity. Nature neuroscience. 2001; 4:1187–1193. [PubMed: 11685225]

Chircop M, Sarcevic B, Larsen MR, Malladi CS, Chau N, Zavortink M, Smith CM, Quan A, Anggono V, Hains PG, Graham ME, Robinson PJ. Phosphorylation of dynamin II at serine-764 is associated with cytokinesis. Biochim. Biophys. Acta. 2011; 1813:1689–1699. [PubMed: 21195118]

Cijsouw T, Weber JP, Broeke JH, Broek JA, Schut D, Kroon T, Saarloos I, Verhage M, Toonen RF. Munc18-1 redistributes in nerve terminals in an activity- and PKC-dependent manner. Journal of cell biology. 2014; 204:759–775. [PubMed: 24590174]

Cingolani LA, Goda Y. Actin in action: the interplay between the actin cytoskeleton and synaptic efficacy. Nature reviews. 2008; 9:344–356.

Cook T, Mesa K, Urrutia R. Three dynamin-encoding genes are differentially expressed in developing rat brain. Journal of neurochemistry. 1996; 67:927–931. [PubMed: 8752097]

Cousin MA, Robinson PJ. The dephosphins: dephosphorylation by calcineurin triggers synaptic vesicle endocytosis. Trends in neurosciences. 2001; 24:659–665. [PubMed: 11672811]

Cremona O, De Camilli P. Synaptic vesicle endocytosis. Current opinion in neurobiology. 1997; 7:323–330. [PubMed: 9232811]

Dittman J, Ryan TA. Molecular circuitry of endocytosis at nerve terminals. Annual review of cell and developmental biology. 2009; 25:133–160.

Faire K, Trent F, Tepper JM, Bonder EM. Analysis of dynamin isoforms in mammalian brain: dynamin-1 expression is spatially and temporally regulated during postnatal development. PNAS. 1992; 89:8376–8380. [PubMed: 1387713]

Ferguson SM, Brasnjo G, Hayashi M, Wolfel M, Collesi C, Giovedi S, Raimondi A, Gong LW, Ariel P, Paradise S, O'Toole E, Flavell R, Cremona O, Miesenbock G, Ryan TA, De Camilli P. A selective activity-dependent requirement for dynamin 1 in synaptic vesicle endocytosis. Science. 2007; 316:570–574. [PubMed: 17463283]

Ferguson SM, De Camilli P. Dynamin, a membrane-remodelling GTPase. Nature reviews. Molecular cell biology. 2012; 13:75–88. [PubMed: 22233676]

Fernandez-Alfonso T, Kwan R, Ryan TA. Synaptic vesicles interchange their membrane proteins with a large surface reservoir during recycling. Neuron. 2006; 51:179–186. [PubMed: 16846853]

Fortin DL, Nemani VM, Voglmaier SM, Anthony MD, Ryan TA, Edwards RH. Neural activity controls the synaptic accumulation of alpha-synuclein. Journal of neuroscience. 2005; 25:10913–10921. [PubMed: 16306404]

Gonzalez-Jamett AM, Momboisse F, Haro-Acuna V, Bevilacqua JA, Caviedes P, Cardenas AM. Dynamin-2 function and dysfunction along the secretory pathway. Frontiers in endocrinology. 2013; 4:126. [PubMed: 24065954]

Graham ME, Anggono V, Bache N, Larsen MR, Craft GE, Robinson PJ. The in vivo phosphorylation sites of rat brain dynamin I. Journal of biological chemistry. 2007; 282:14695–14707. [PubMed: 17376771]

Gray NW, Fourgeaud L, Huang B, Chen J, Cao H, Oswald BJ, Hemar A, McNiven MA. Dynamin 3 is a component of the postsynapse, where it interacts with mGluR5 and Homer. Current biology. 2003; 13:510–515. [PubMed: 12646135]

Gray NW, Kruchten AE, Chen J, McNiven MA. A dynamin-3 spliced variant modulates the actin/cortactin-dependent morphogenesis of dendritic spines. Journal of cell science. 2005; 118:1279–1290. [PubMed: 15741233]

Gundelfinger ED, Kessels MM, Qualmann B. Temporal and spatial coordination of exocytosis and endocytosis. Nature reviews. 2003; 4:127–139.

Han EB, Stevens CF. Development regulates a switch between post- and presynaptic strengthening in response to activity deprivation. PNAS. 2009; 106:10817–10822. [PubMed: 19509338]

Ishida N, Nakamura Y, Tanabe K, Li SA, Takei K. Dynamin 2 associates with microtubules at mitosis and regulates cell cycle progression. Cell structure and function. 2011; 36:145–154. [PubMed: 21150131]

Kurklinsky S, Chen J, McNiven MA. Growth cone morphology and spreading are regulated by a dynamin-cortactin complex at point contacts in hippocampal neurons. Journal of neurochemistry. 2011; 117:48–60. [PubMed: 21210813]

Liu JP, Sim AT, Robinson PJ. Calcineurin inhibition of dynamin I GTPase activity coupled to nerve terminal depolarization. Science. 1994; 265:970–973. [PubMed: 8052858]

Liu YW, Surka MC, Schroeter T, Lukiyanchuk V, Schmid SL. Isoform and splice-variant specific functions of dynamin-2 revealed by analysis of conditional knockout cells. Molecular biology of the cell. 2008; 19:5347–5359. [PubMed: 18923138]

Lu J, Helton TD, Blanpied TA, Racz B, Newpher TM, Weinberg RJ, Ehlers MD. Postsynaptic positioning of endocytic zones and AMPA receptor cycling by physical coupling of dynamin-3 to Homer. Neuron. 2007; 55:874–889. [PubMed: 17880892]

Marks B, McMahon HT. Calcium triggers calcineurin-dependent synaptic vesicle recycling in mammalian nerve terminals. Current biology. 1998; 8:740–749. [PubMed: 9651678]

McPherson PS, Takei K, Schmid SL, De Camilli P. p145, a major Grb2-binding protein in brain, is co-localized with dynamin in nerve terminals where it undergoes activity-dependent dephosphorylation. Journal of biological chemistry. 1994; 269:30132–30139. [PubMed: 7982917]

Mettlen M, Pucadyil T, Ramachandran R, Schmid SL. Dissecting dynamin's role in clathrin-mediated endocytosis. Biochemical Society transactions. 2009; 37:1022–1026. [PubMed: 19754444]

Mueller VJ, Wienisch M, Nehring RB, Klingauf J. Monitoring clathrin-mediated endocytosis during synaptic activity. Journal of neuroscience. 2004; 24:2004–2012. [PubMed: 14985443]

Nelson JC, Stavoe AK, Colon-Ramos DA. The actin cytoskeleton in presynaptic assembly. Cell adhesion & migration. 2013; 7:379–387. [PubMed: 23628914]

Noda Y, Nakata T, Hirokawa N. Localization of dynamin: widespread distribution in mature neurons and association with membranous organelles. Neuroscience. 1993; 55:113–127. [PubMed: 8350983]

O'Brien RJ, Kamboj S, Ehlers MD, Rosen KR, Fischbach GD, Huganir RL. Activity-dependent modulation of synaptic AMPA receptor accumulation. Neuron. 1998; 21:1067–1078. [PubMed: 9856462]

Pozo K, Goda Y. Unraveling mechanisms of homeostatic synaptic plasticity. Neuron. 2010; 66:337–351. [PubMed: 20471348]

Presek P, Jessen S, Dreyer F, Jarvie PE, Findik D, Dunkley PR. Tetanus toxin inhibits depolarization-stimulated protein phosphorylation in rat cortical synaptosomes: effect on synapsin I phosphorylation and translocation. Journal of neurochemistry. 1992; 59:1336–1343. [PubMed: 1328520]

Raimondi A, Ferguson SM, Lou X, Armbruster M, Paradise S, Giovedi S, Messa M, Kono N, Takasaki J, Cappello V, O'Toole E, Ryan TA, De Camilli P. Overlapping role of dynamin isoforms in synaptic vesicle endocytosis. Neuron. 2011; 70:1100–1114. [PubMed: 21689597]

Robinson PJ, Liu JP, Powell KA, Fykse EM, Sudhof TC. Phosphorylation of dynamin I and synaptic-vesicle recycling. Trends in neurosciences. 1994; 17:348–353. [PubMed: 7526507]

Smillie KJ, Cousin MA. Dynamin I phosphorylation and the control of synaptic vesicle endocytosis. Biochemical Society symposium. 2005:87–97. [PubMed: 15649133]

Tan TC, Valova VA, Malladi CS, Graham ME, Berven LA, Jupp OJ, Hansra G, McClure SJ, Sarcevic B, Boadle RA, Larsen MR, Cousin MA, Robinson PJ. Cdk5 is essential for synaptic vesicle endocytosis. Nature cell biology. 2003; 5:701–710. [PubMed: 12855954]

Tanifuji S, Funakoshi-Tago M, Ueda F, Kasahara T, Mochida S. Dynamin isoforms decode action potential firing for synaptic vesicle recycling. Journal of biological chemistry. 2013; 288:19050–19059. [PubMed: 23687302]

Turrigiano GG, Leslie KR, Desai NS, Rutherford LC, Nelson SB. Activity-dependent scaling of quantal amplitude in neocortical neurons. Nature. 1998; 391:892–896. [PubMed: 9495341]

Urrutia R, Henley JR, Cook T, McNiven MA. The dynamins: redundant or distinct functions for an expanding family of related GTPases? PNAS. 1997; 94:377–384. [PubMed: 9012790]

van der Bliek AM. Functional diversity in the dynamin family. Trends in cell biology. 1999; 9:96–102. [PubMed: 10201074]

Verstegen AM, Tagliatti E, Lignani G, Marte A, Stolero T, Atias M, Corradi A, Valtorta F, Gitler D, Onofri F, Fassio A, Benfenati F. Phosphorylation of synapsin I by cyclin-dependent kinase-5 sets the ratio between the resting and recycling pools of synaptic vesicles at hippocampal synapses. Journal of neuroscience. 2014; 34:7266–7280. [PubMed: 24849359]

Wondolowski J, Dickman D. Emerging links between homeostatic synaptic plasticity and neurological disease. Frontiers in cellular neuroscience. 2013; 7:223. [PubMed: 24312013]

Xue J, Graham ME, Novelle AE, Sue N, Gray N, McNiven MA, Smillie KJ, Cousin MA, Robinson PJ. Calcineurin selectively docks with the dynamin Ixb splice variant to regulate activity-dependent bulk endocytosis. Journal of biological chemistry. 2011; 286:30295–30303. [PubMed: 21730063]

Zhang W, Benson DL. Developmentally regulated changes in cellular compartmentation and synaptic distribution of actin in hippocampal neurons. Journal of neuroscience research. 2002; 69:427–436. [PubMed: 12210837]

Highlights

- The distribution of endogenous dynamins 1, 2, and 3 were studied in cultured hippocampal neurons.
- Dyn3 accumulates in, and Dyn1 disperses from, nerve terminals during chronic neuronal silencing.
- Silencing-induced Dyn3 clustering is actin-independent and slower than synapsin clustering.
- Dyn3 synaptic clustering is regulated by the calcium-dependent protein phosphatase calcineurin.

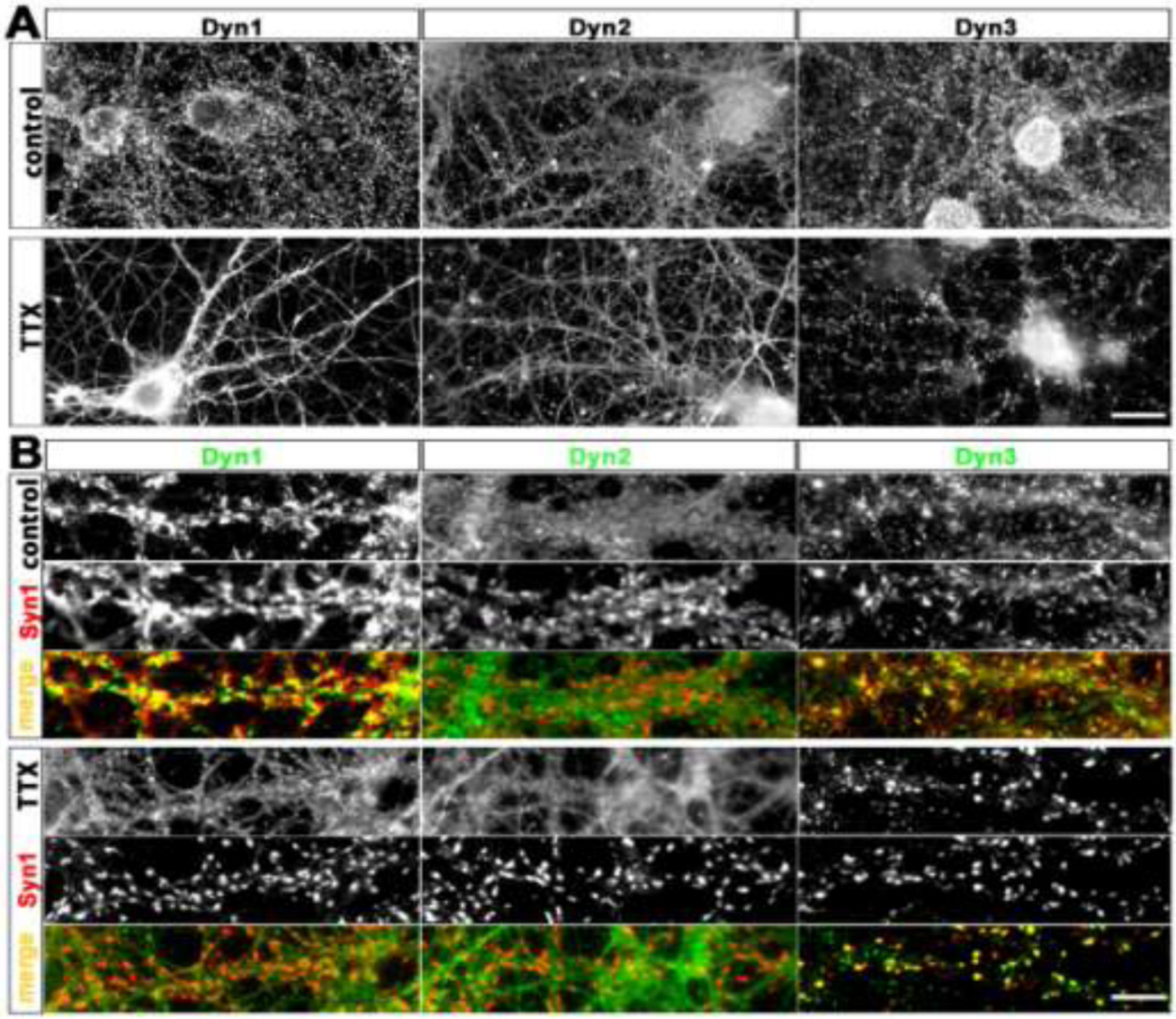

Fig. 1. Distribution of endogenous dynamins in cultured hippocampal neurons before and after chronic suppression of neural activity

Hippocampal cultures were fixed at 21 DIV and stained using isoform-specific antibodies to Dyn1, 2, and 3, as indicated.

A. Under control conditions endogenous Dyn1 is detectable in a punctate manner along the dendritic arbor, axons and nerve terminals of a 21 DIV hippocampal neuron. Endogenous Dyn2 is detectable in a mostly diffuse pattern throughout all neuronal compartments, and not enriched at synaptic sites. Dyn3 immunoreactivity is characterized by fine puncta present throughout the neurons, with occasional enrichment at some presumptive synapses. Chronic incubation with TTX (1 μM, 14 days) causes an apparent declustering of Dyn1, no detectable change in Dyn2 localization, and a marked accumulation of Dyn3 into larger clusters. Scale bar: 15 μM. **B.** Selected dendritic regions from hippocampal neurons cultured with or without TTX, immunostained with the presynaptic marker Syn1, together with each

indicated dynamin isoforms. Note that the apparent degree of colocalization between Syn1 and Dyn1 increases with TTX, but Syn colocalization with Dyn3 decreases. Scale bar: 8 μM.

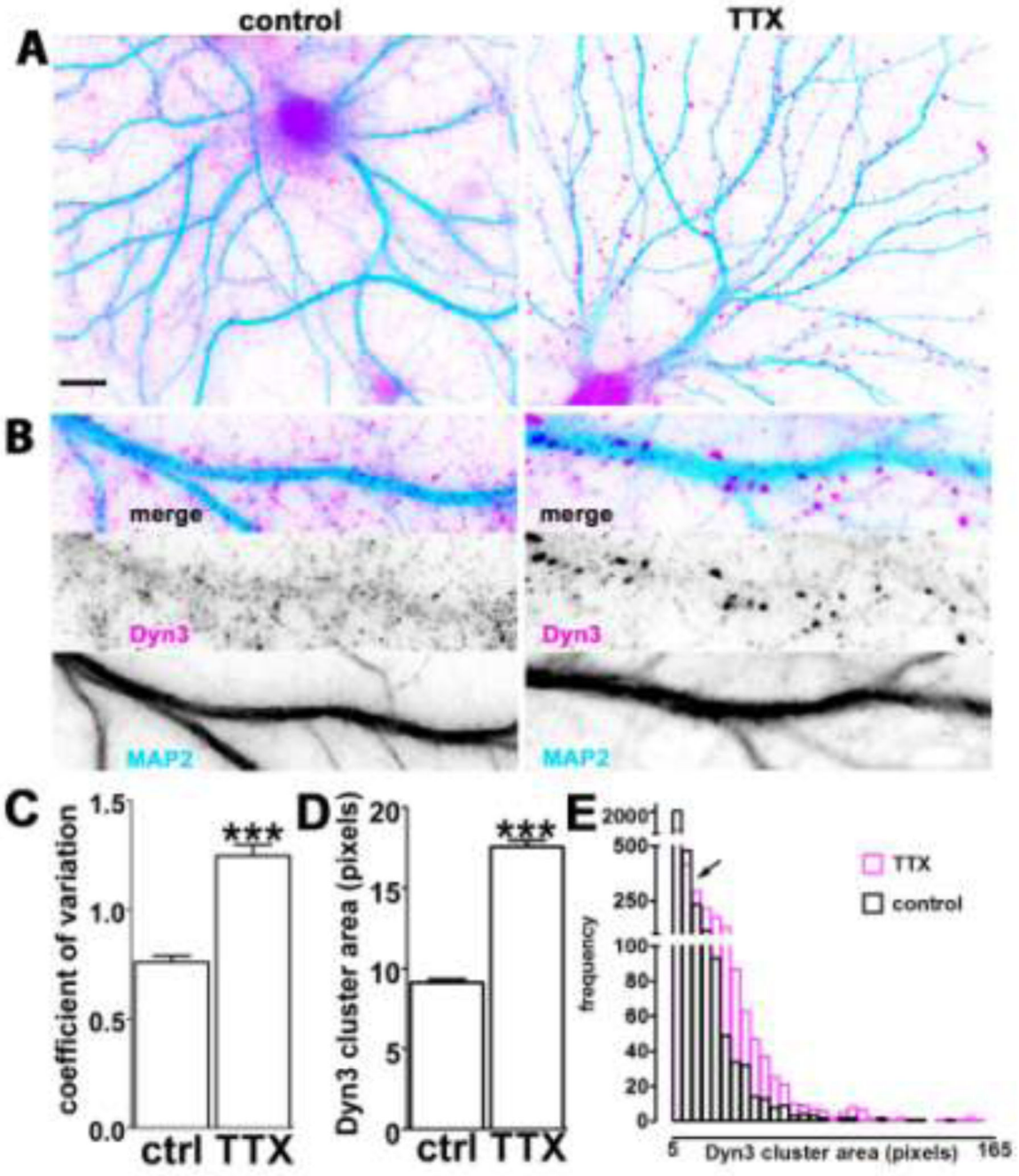

Fig. 2. Dyn3 clustering is accompanied by a decrease in small diffuse puncta

A. Representative hippocampal neurons incubated in the absence (*left*) or presence (*right*) of TTX for 2 weeks, prior to double immunostaining for Dyn3 (*magenta*) and MAP2 (*light blue*) to highlight the dendritic arborization. Scale bar: 10 μM. **B.** Selected dendritic regions from 21 DIV hippocampal neurons, cultured with or without TTX and stained with anti-Dyn3 antibody (*magenta*) and anti-MAP2 (*light blue*). Image width: 35 μM. **C.** Comparison of the variability of pixel intensity for Dyn3, expressed as coefficient of variation of pixel intensity values (see the Experimental methods section for details) indicates that TTX (14

days) generates Dyn3 immunoreactivity that is less diffuse and more concentrated at particular locations (number of dendritic regions = 12 for each group, *** $p<0.001$; unpaired t-test). **D.** Quantification of Dyn3 cluster size after incubation with TTX (14 days). The data are expressed as mean ± SEM (*** $p<0.001$ unpaired t-test; number of clusters: control, 3150; TTX, 2329). **E.** Frequency histograms of Dyn3 cluster area in control (*black*) and after TTX (*purple*); bin size = 5 pixels. *Black arrow* indicates the part of the histogram where TTX shifts Dyn3 cluster size distribution from favoring clusters smaller than 10 pixels to those larger than 10 pixels.

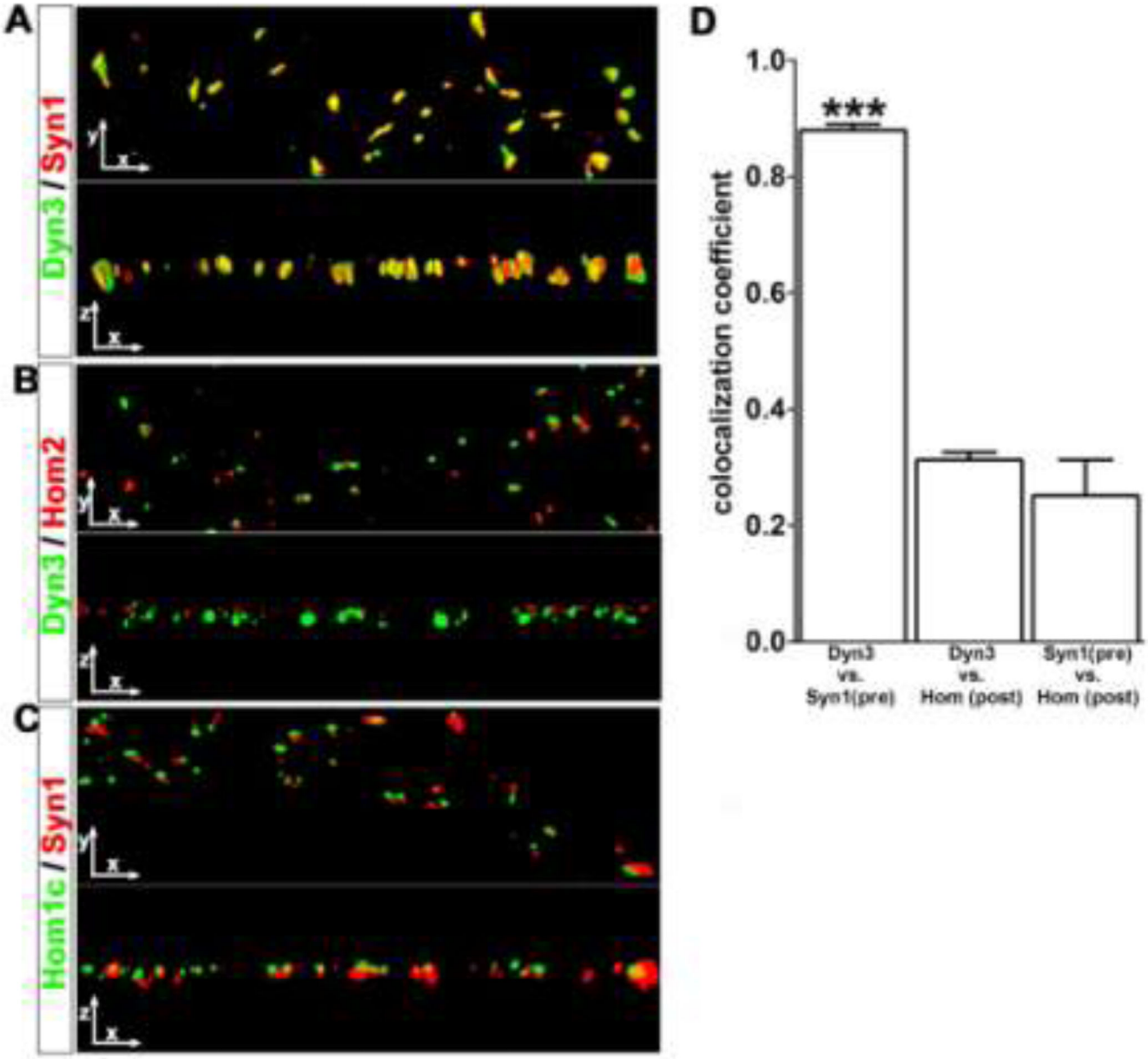

Fig. 3. TTX-induced Dyn3 clusters colocalize with pre-, not post-synaptic markers

A–C. Three-dimensional surface renderings of dendritic regions, stained for Dyn3, Syn1, Homer 2 and Homer1c, as indicated, at 0 and 90 degree rotations after Z-series image collection and image deconvolution. In yellow regions of colocalization. Image width: 30 μM. **D.** The coefficient of colocalization between Dyn3 and Syn1 (0.87 ± 0.01, number of dendritic regions=15) was significantly higher than the coefficient of colocalization between Dyn3 and Homer (0.3124 ± 0.01, number of dendritic regions=8, $p<0.001$ one-way ANOVA, and Tukey's multiple comparison post hoc test), or Syn1 and Homer (0.25 ± 0.06, number of dendritic regions =15, $p<0.001$ one-way ANOVA, Tukey's multiple comparison test).

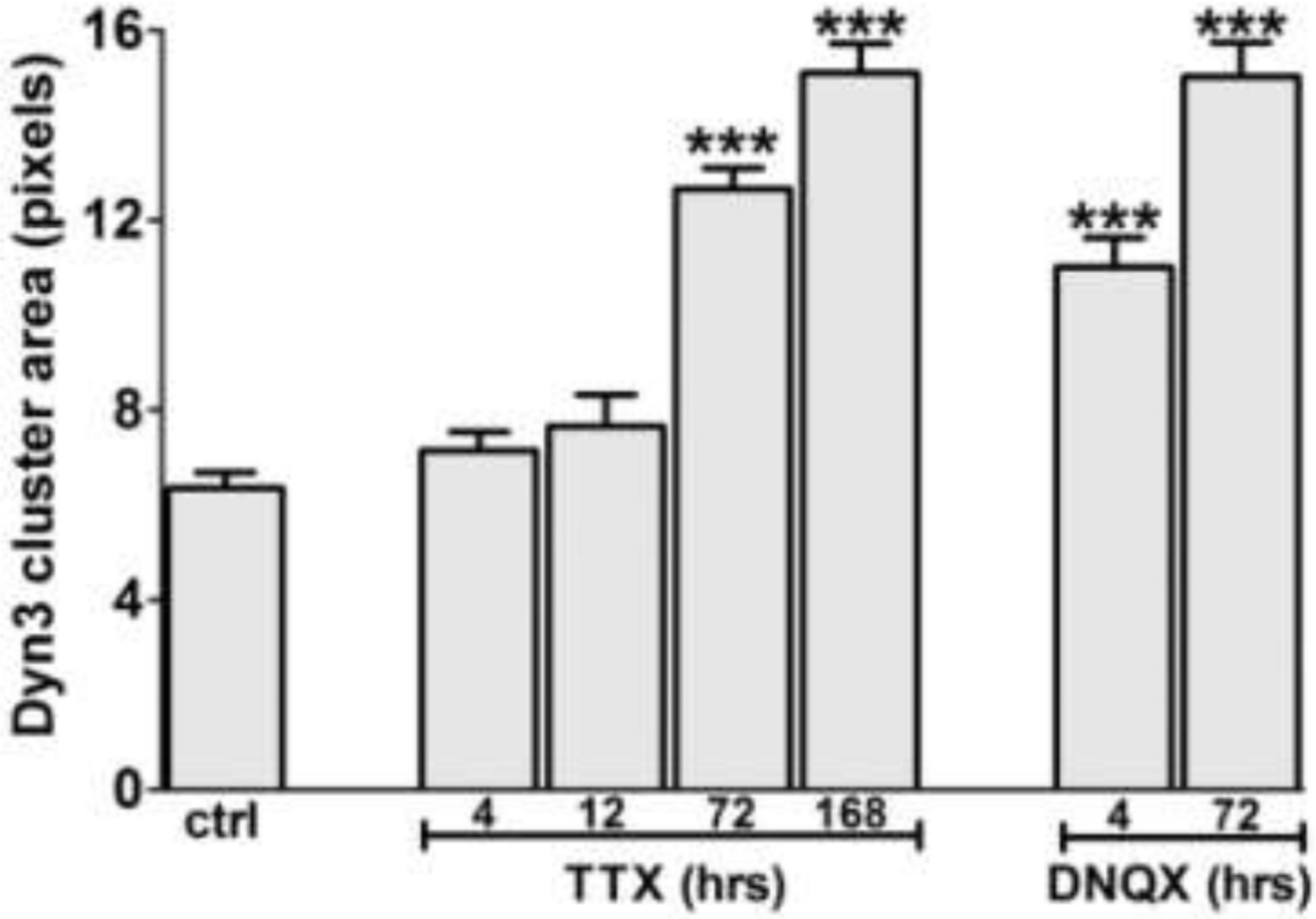

Fig. 4. Different time-course of TTX- and DNQX-induced Dyn3 clustering

Quantification of Dyn3 clustering after different incubation times with 1 μM TTX or 20 μM DNQX. The data are expressed as mean ± SEM of cluster area (number of clusters= control, 218; 4 h TTX, 185; 12 h TTX, 123; 3 days TTX, 758; 7 days TTX, 519; 4 h DNQX, 265; 3 days DNQX, 454. *** $p<0.01$,one-way ANOVA, followed by Dunnett's test).

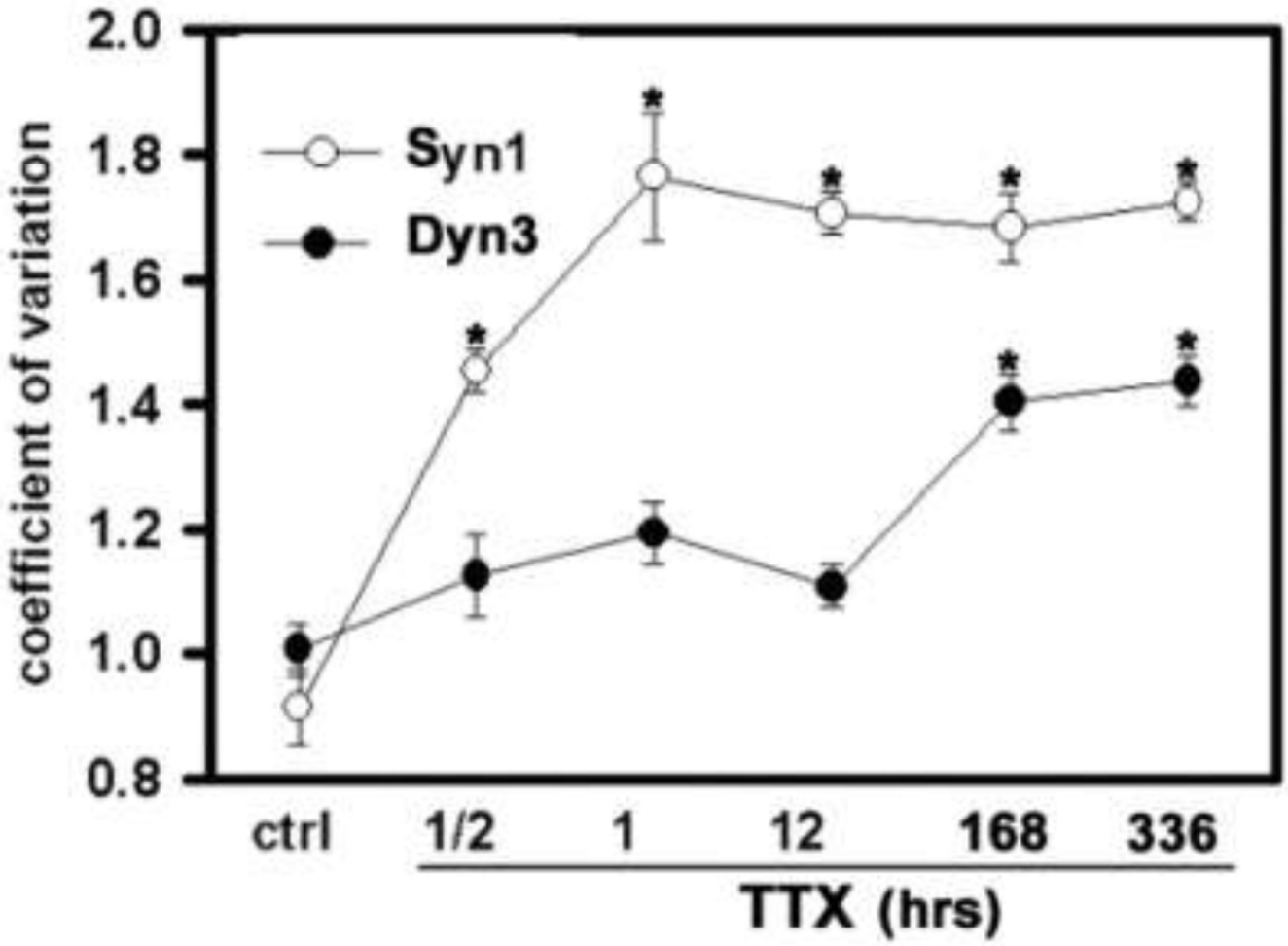

Fig. 5. Different time-course of Dyn3 and Syn1 TTX-induced clustering

Quantification of Dyn3 and Syn1 clustering after different incubation time with 1 μM TTX. The effect of TTX on the redistribution of the two proteins is calculated as coefficient of variation of pixel intensity (see the Experimental methods section for details). Number of dendritic regions: control, 8 (Dyn3), 8 (Syn1); ½ h TTX, 12 (Dyn3), 9 (Syn1); 1 h TTX, 15 (Dyn3), 8 (Syn1); 12 h TTX, 12 (Dyn3), 8 (Syn1); 7 days TTX, 9 (Dyn3), 9 (Syn1); 14 days TTX, 14 (Dyn3), 14 (Syn1). *$p<0.001$, one-way ANOVA, and Dunnett's multiple comparison tests.

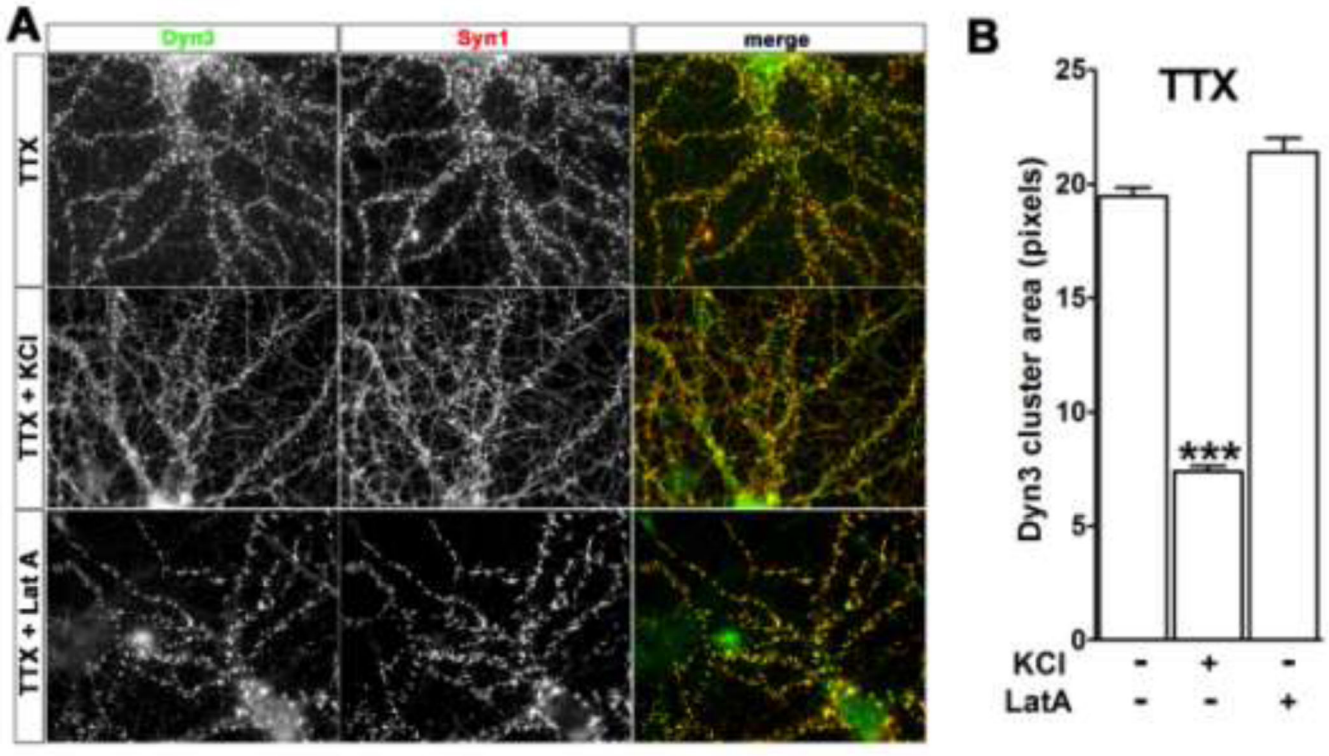

Fig. 6. Depolarization induces Dyn3 de-clustering

A. Hippocampal neurons were pre-incubated for 2 weeks with 1 μM TTX to induce Dyn3 clustering, and then incubated in the absence or presence of either 20 mM KCl for 5 min, or 50 μM Latrunculin A (Lat-A) for 20 min, as indicated, prior to immunostaining for Syn1 and Dyn3. Image width: 100 μM. **B.** Quantification of the area of Dyn3 clusters in the different conditions indicated above. Data are expressed as mean + SEM (*** $p<0.001$ number of clusters: 2327 (TTX); 4964 (TTX/KCl); 1762 (TTX/LatA)).

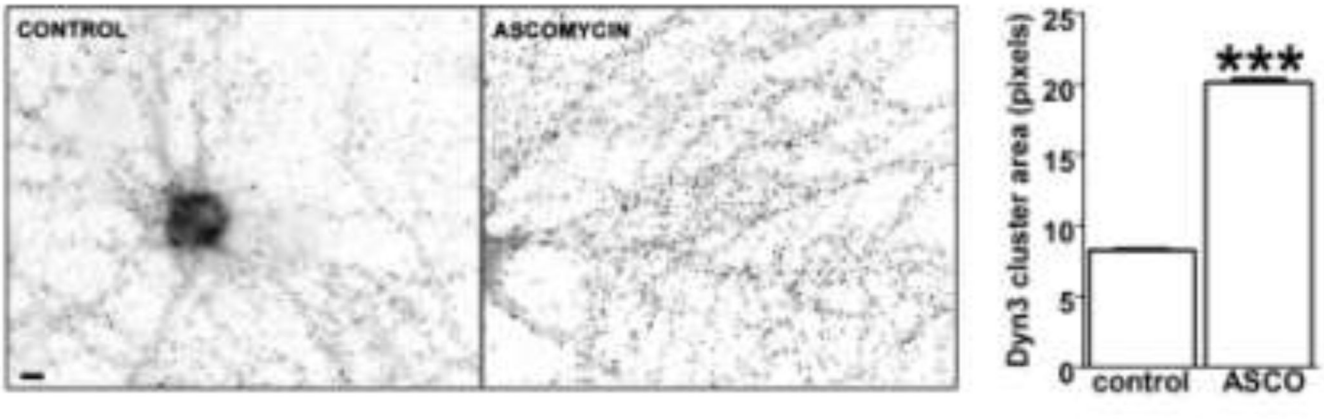

Fig. 7. Calcineurin antagonist ascomycin increases Dyn3 clustering

Hippocampal neurons stained with anti-dynamin3 antibody in the absence (*left*) or presence (*right*) of 0.5 μM ascomycin for 1 hour. (number of clusters = 6130 (control); 7735 (ascomycin), *** $p<0.001$; unpaired t-test). Scale bar: 5 μM.